

A microfluidic platform for sequential ligand labeling and cell binding analysis

Guodong Sui · Cheng-Chung Lee · Ken-Ichiro Kamei ·
Hua-Jung Li · Jin-Yi Wang · Jun Wang ·
Harvey R. Herschman · Hsian-Rong Tseng

Published online: 29 December 2006
© Springer Science + Business Media, LLC 2007

Abstract Developing biochemical and cell biological assay for screening biomolecules, evaluating their characteristics in biological processes, and determining their pharmacological effects represents a key technology in biomedical research. A PDMS-based integrated microfluidic platform was fabricated and tested for facilitating the labeling of ligand on the nanogram scale and sequential cell binding analysis in a manner that saves both time and reagents. Within this microfluidic platform, ligand labeling, cell immobilization, and optical analysis are performed in a miniaturized, continuous and semi-automated manner. This microfluidic device for ligand labeling and cell analysis is composed of two functional modules: (i) a circular reaction loop for fluorophore-labeling of the ligand and (ii) four parallel-oriented incubation chambers for immobilization of cells, binding of ligand to different cell populations, and optical evaluation of interactions between the labeled ligand and its cell targets. Epidermal growth factor (EGF) as the ligand and different cell lines with various levels of EGF receptor expression have been utilized to test the feasibility of this microfluidic platform. When compared to studies with traditional Petri dish handling of cells and tissues, or even microwell analyses, experiments with the microfluidic platform described here are much less time consuming, conserve reagents, and are programmable,

which makes these platforms a very promising new tool for biological studies.

Keywords Microfluidics · Ligand labeling · PDMS · EGF · EGFR

Introduction

The development of biochemical and cell biological assays (Khandurina and Guttman, 2002) for screening of biomolecules, evaluating their characteristics in biological processes, and determining their pharmacological effects represents a key technology in biomedical research. Assays that employ incubation of cells with fluorescently labeled probes, followed by microscopic evaluation, are commonly used in cell biology (Abraham et al., 2004). These assays often require a considerable quantity of the biomolecules (hormone, ligand, growth factor, antibody, etc.), because the fluorophore-labeling reaction is performed at a macroscopic level. To conserve such reagents it is both desirable and challenging (Abraham et al., 2004) to perform fluorophore-labeling reactions on nanogram (ng) or picogram (pg) scales. In addition, the use of conventional screening platforms such as 96-well plates consumes significant amounts of probe, because a few microliters (μL) of probe solution is needed, at a minimum, to fill each screening well. Although many fluorescent probes are commercially available, the lack of nanoscale methods for performing both the fluorophore-labeling reaction and the sequential cell assays compromises the feasibility of performing these cell biological assays when the probe molecule is the limiting resource in a biological system. To develop miniaturized and more efficient operational platforms for performing cell-based assays, using small quantities of fluorescent probes, would be of great value in such contexts.

G. Sui · K.-I. Kamei · H.-J. Li · J.-Y. Wang · J. Wang ·
H. R. Herschman (✉) · H.-R. Tseng (✉)
Department of Molecular Medical Pharmacology and Crump
Institute for Molecular Imaging, University of California, Los
Angeles, 700 Westwood Plaza,
Los Angeles, CA 90095, USA
e-mail: hherschman@mednet.ucla.edu
e-mail: hrtseng@mednet.ucla.edu

C.-C. Lee
Department of Bioengineering, California Institute of Technology,
Pasadena, CA 90095, USA

Poly(dimethylsiloxane) (PDMS)-based integrated microfluidic systems (Groisman et al., 2003) provide powerful platforms for integrating syntheses, bioassays, and optical measurements because of (i) rapid kinetics (Worz et al., 2001) and fast mass and heat transfer (Bird et al., 2002; Watts and Haswell, 2003) within the microfluidic environment, (ii) reduced consumption of reagents, solutions, and biological samples, (iii) feasibility of integrating chemical, biological, and analytical processes on a single device, (iv) the ability to perform direct optical measurements as a result of the transparent nature of PDMS matrixes, (McDonald and Whitesides, 2002) and (v) the gas permeability that allows gas exchange between enclosed microchambers and the surrounding environment (Hung et al., 2005). Furthermore, the low elastic modulus of PDMS materials (Merkel et al., 2000) permits the parallel fabrication of functional modules to perform isolation, metering, active mixing, and trapping processes, all within a single device (Liu et al., 2003). A number of systems have been devised that use such functional modules within microfluidic devices, including polymerase chain reaction (PCR) devices, (Liu et al., 2003) miniaturized DNA sequencers, (Braslavsky et al., 2003; Reese et al., 2003) protein crystallization chambers, (Hansen et al., 2004) highly integrated memory devices (Thorsen et al., 2002) and reaction circuits for multistep synthesis (Lee et al., 2005).

We demonstrate here a new type of PDMS-based microfluidic platform (Fig. 1), within which we both prepare a fluorophore-labeled ligand on the ng scale and perform cell binding assays with the fluorescent ligand on living cells. Ligand labeling, cell binding, and optical analysis are performed in a miniaturized, continuous and semi-automated manner. The microfluidic device for ligand labeling and cell analysis is composed of two functional modules: (i) a circular reaction loop for fluorophore-labeling of the ligand and (ii) four parallel-oriented incubation chambers for immobilization of cells, binding of ligand to different cell populations, and optical evaluation of interactions between the labeled ligand and its cell targets.

To test the operation of this microfluidic platform, we used the epidermal growth factor (EGF)/epidermal growth factor receptor (EGFR) signaling system (EI-Rayes and LoRusso, 2004). EGF is a small mitogenic protein with 53 amino acids in length. EGF mediates biological processes that include cell growth, oncogenesis, and wound healing (Aharonov et al., 1977). The EGF/EGFR signal transduction pathway regulates cell growth, proliferation, and differentiation, all of which are critical for maintaining morphological and functional homeostasis of tissues, primarily those of epithelial origin (Herbst, 2004). The EGF/EGFR signaling system is highly regulated in normal tissues, but is often deregulated in epithelial tumors. EGF receptors are often over-expressed and/or mutated in tumors, leading to aggressive tumor growth, resistance to standard treatment protocols and

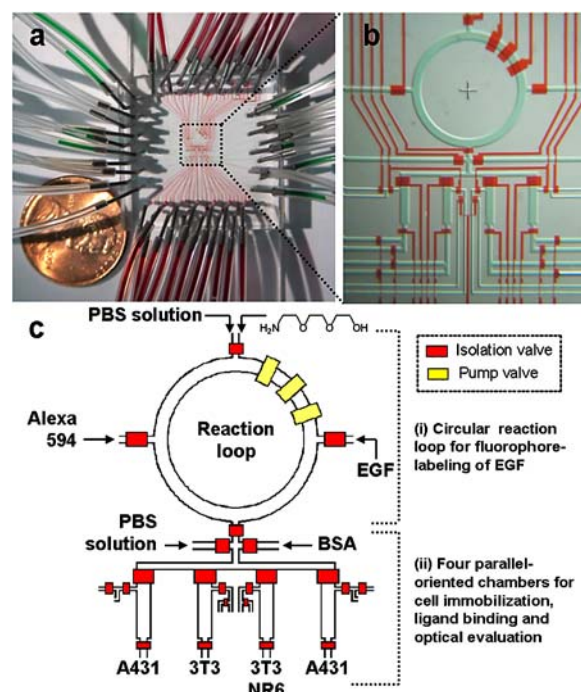


Fig. 1. (a) Photo of the microfluidic chip used for EGF-labeling and cell binding studies. (b) Optical micrograph of the central area of the chip. The various channels are loaded with food dyes to help visualize the different layers of the microfluidic chip: Green for fluidic channels and Red for control channels. (c) Schematic representation of the two functional modules of the microfluidic chip: (i) the top circular reaction loop and (ii) the bottom four cell incubation chambers. The operation of the microfluidic chip is controlled by pressure-driven valves; delegated responsibilities are illustrated by their colors. Red identifies regular valves for controlling flow of solutions containing reagents and cells; yellow identifies circulation pump valves for active mixing inside the reaction loop

substantially decreased patient survival (Nair, 2005). The presence of over-expressed and/or mutant EGF receptors is now used diagnostically for clinical evaluation of patients, and over-expressed and/or mutated EGF receptors have become molecular targets for targeted cancer therapeutics.

Materials and methods

Microfluidic chip fabrication

The chip was fabricated using multi-layer soft lithography. Two different molds were first fabricated by photolithographic processes to create the fluidic channels and the control channels for actuating the valves located in the respective layers of the PDMS-based microfluidic chip. The mold used to create the fluidic channels was made by spin-coating a layer of 30- μm thick positive photoresist (AZ 100XT PLP) on the silicon wafer (Silicon Quest, San Jose, USA). After UV exposure and development, the wafer was heated above

the glass transition temperature of the positive photoresist. As a result, the surface profile of the patterned positive photoresist was transformed into a round profile. This device has a channel height of 30 μm and width of 50–400 μm . The control channel mold was made by fabricating a 25 μm -thin negative photoresist (SU8-2025) pattern on a silicon wafer.

Before fabricating the device, both the fluidic and control molds were exposed to trimethylchlorosilane (TMSCl) vapor for 2–3 min. Well-mixed PDMS (GE, RTV 615 A and B in 5:1 ratio) was poured onto the fluidic mold located in a Petri dish to give a 5 mm-thick fluidic layer. Another portion of PDMS (GE, RTV 615 A and B in 20:1 ratio) was spin-coated onto the control mold (1600 rpm, 60 s, ramp 15 s) to obtain the control layer. The thick fluidic layer and thin control layer were cured in an 80°C oven for 50 min. After incubation, the thick fluidic layer was peeled off the mold, and holes were punched onto the fluidic layer for access of reaction solutions. The fluidic layer was then trimmed, cleaned and aligned onto the thin control layer. After baking at 80°C for 60 min, the assembled layer was peeled off the control mold, and another set of holes were punched for access to control channels. These assembled layers were then placed on top of a glass slide that was coated (1600 rpm, 60 s, ramp 15 s) with PDMS (GE RTV 615 A and B in 20:1 ratio) that had been cured for 45 min in the oven. The device was complete after overnight incubation.

Control interface

The pneumatic control setup consists of 4 sets of eight-channel manifolds controlled through BOB3 breakout controller board (Fluidigm, San Francisco, USA). 32 Control lines from the device are individually connected to the corresponding channels on the manifolds with metal pins (23 Gauge, New England Small Pin Corp, USA) using Tygon microbore tubing (Cole-Parmer East, Bunker Court, USA). When a channel on the manifold is activated, argon gas enters the control line connected to the specific channel, providing pressure to close valves in the microfluidic device. The control interface was created using LabVIEW program on a PC. A digital I/O card (AT-DIO-32HS National Instruments) controls the switching of manifolds through the BOB3 breakout controller board. The LabVIEW program allows for manual control of individual valves and for semi-automation of the whole experiment processes.

Cell preparation

The NIH-3T3 murine fibroblast cell line and the A431 human epidermoid carcinoma cell line were obtained from the American Type Culture Collection (Manassas, VA). The 3T3-NR6 cell line was established by using the procedure described by Pruss and Herschman (1977) The NIH-3T3,

A431, and 3T3-NR6 cells were grown in Dulbecco's Modified Eagle Medium (DMEM), containing heat-inactivated 10% calf serum (CS), 0.2 mM glutamine, and 100 units/mL penicillin and 100 mg/mL streptomycin (PS) at 37°C in a humidified incubator (95% air, 5% CO₂). The cell lines were passaged at 80–90% confluence. The cells (with a concentration of 1–10⁷ cells/mL), suspended in DMEM with PS and glutamine, were injected into the microfluidic device to perform the experiment.

Image analysis

Light and fluorescent micrographs were taken by Zeiss Axioskop 2 fluorescent microscopy (Zeiss, Germany). All fluorescent images employed for protein repelling investigation were taken using the same objective (10 \times), with an identical exposure time of 5 s.

Results and discussions

Our microfluidic device, fabricated with soft-lithography methods, is based on a two-layer design that uses a push-up valve configuration (Unger et al., 2000). Valves are created at the points where fluidic channels and control channels overlap and the fluid channel and control channel are separated only by a thin elastic membrane. By applying a positive pressure in the control channel, the thin membrane deflects upward, pinching off the fluid path, thus closing the valve. Figure 1(a) and (b) display optical micrographs of the microfluidic devices. For this image, the various channels were loaded with food dyes to facilitate visualization of the upper fluidic channels (filled with GREEN dye) which host the cell lines and transport alternative reagents for various experiments, and the lower control layer (filled with RED dye) which is responsible for opening and closing of the valves. Among the valves (Fig. 1(c)), the three sequentially arranged rectangles on the upper-right-hand side of the circular loop constitute a circulating pump that can close and open in a controlled sequence to improve the efficacy of reagent mixing in the fluidic channels.

Using this microfluidic device, we performed fluorescent EGF binding assays on three cell lines. A431 cells are a human epidermoid carcinoma cell line that have an amplified EGFR gene, and express 1–2 $\times 10^6$ receptors per cell. 3T3 cells are immortalized murine fibroblasts that express 50,000–100,000 EGF receptors per cell. 3T3-NR6 cells are derived from 3T3 cells; they express no detectable EGF receptor message or EGF receptor protein. By manually controlling the isolation valves, the four chambers of the microfluidic device were filled separately with the A431, 3T3, 3T3-NR6, and A431 cells as shown in the diagram of Fig. 1(c). To immobilize the cells on the channel surfaces, so they

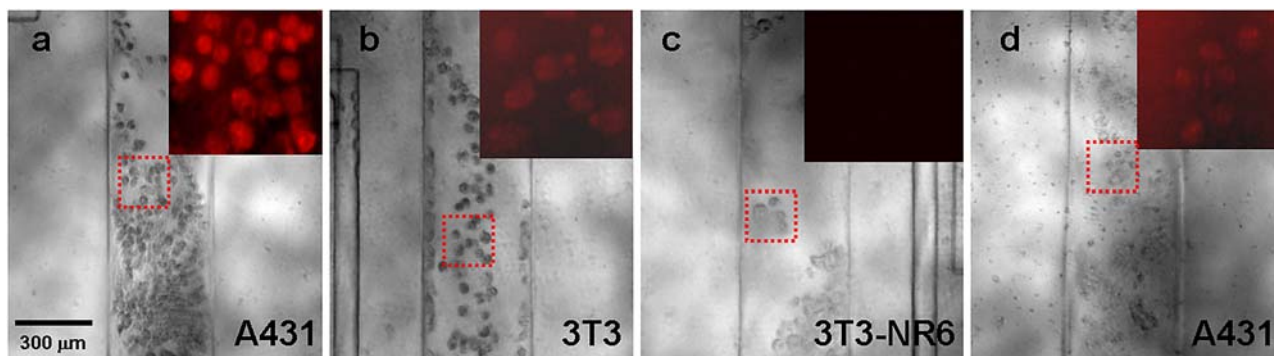


Fig. 2 Light and fluorescent micrographs (insets) of cultured cells taken after exposure to on-chip synthesized Alexa-labeled EGF and subsequent washing (a)–(c) A competition experiment was performed

with unlabeled EGF to rule out non-specific ligand binding (d). The red dashed boxes indicate that the location where the respective fluorescent micrographs were taken

would not flow out during the labeling and washing steps, the PDMS chambers were first coated with fibronectin by introducing a 0.1% fibronectin solution into the chambers and maintaining the device at 25°C for 5 h. After flushing the chambers with cell culture medium, the individual cell lines (ca. 200 cells per chamber) were loaded separately into the respective microfluidic chambers. After incubation for 6 h at 37°C unattached cells were removed with cell culture medium. A phosphate-buffered saline (PBS) solution of bovine serum albumin (BSA) was then passed through each chamber, to prevent subsequent nonspecific binding of fluorescent-labeled EGF to the chamber and cells. After BSA exposure, the chambers were rewashed with PBS. Each washing process took 5 min with a loading pressure of ca. 5 psi.

EGF labeling with the fluorophore (Alexa Fluoro® 594, Invitrogen) was performed in the circular reaction loop in an automated fashion. 15 A 100 $\mu\text{g}/\text{mL}$ solution of EGF (3.0 ng, 0.48 pmol) in PBS (30 nL) was first loaded into the reaction loop from the input channel, followed by introduction of a solution (145 $\mu\text{g}/\text{mL}$, 5 nL) of Alexa 594 (0.73 ng, 0.89 pmol). After closing the isolation valves associated with the reaction loop, the mixing pumps began to sequentially circulate and mix the two solutions inside the reaction loop. After 2 min, a PBS solution (27 $\mu\text{g}/\text{mL}$, 5 nL) of 2-[2-(2-aminoethoxy)ethoxy]ethanol (0.135 ng, 0.90 pmol) was added into the reaction loop to react with any excess (unreacted) Alexa 594. The resulting Alexa-labeled EGF solution (40 nL, 84.9 $\mu\text{g}/\text{mL}$), was then distributed in 10 nL aliquotes into the four incubation chambers, containing the three cell lines. After a five-minute incubation at room temperature between the cell lines and the Alexa-labeled EGF solution, the chambers were washed with cell culture medium to remove unbound labeled ligand. The 4th chamber, containing A431 cells, was then washed with a continuous stream (flow rate: ca. 7 nL/sec) of unlabeled EGF solution (100 $\mu\text{g}/\text{mL}$, total volume: 2 μL), to compete away the bulk of uninternalized EGF on the surface of these cells. Light and fluorescent im-

ages of the resulting four microchambers were then observed microscopically and photographed (Nikon TE-2000, images processed by MetaMorph). Channel coating and cell immobilization were performed on a digitally controlled heater at 37°C in an ambient environment, while fluorescent labeling of EGF and the cell binding analyses were carried out at room temperature (ca. 20°C).

Figure 2 presents light and fluorescent micrographs from each microfluidic chamber, recorded after exposure of the various cell lines to the on-chip synthesized Alexa-labeled EGF. A431 cells in the 1st chamber, which express large numbers of EGF receptors, are clearly distinguished from the background in the fluorescent micrograph with an intense fluorescent signal (Fig. 2(a)), demonstrating successful labeling with Alexa-EGF. In contrast, A431 cells inside the 4th chamber, which was quickly flushed with excess unlabeled EGF after labeling with Alexa-EGF, appear either unlabeled or are discernable by a staining level only slightly above background. The slight staining (Fig. 2(d)) observed on A431 cells in the 4th chamber is likely to result from the small degree of Alexa-EGF internalization (and thus sequestration) that occurred prior to competition with unlabelled EGF. These competition data with unlabelled EGF suggest that non-specific ligand binding (at least for EGF) is not a significant problem in this microfluidic cell labeling device.

As a second method of evaluation of non-specific labeling of EGF receptors with fluorescent EGF in the microfluidic platform we compared labeling of 3T3 cells, which have “normal” levels of EGF receptors and 3T3-NR6 cells, which have no detectable EGF receptor or EGF receptor mRNA. The fluorescent signal intensity (Fig. 2(b)) of Alexa-EGF labeled 3T3 cells inside the 2nd chamber is much lower than that of A431 cells in the 1st chamber, but is clearly discernable. In contrast, no significant signal (Fig. 2(c)) can be observed from the 3T3-NR6 cells exposed to Alex-EGF inside the 3rd chamber. These data, like the data with A431 cells, demonstrate the specific

labeling of cells expressing EGF receptors with fluorescent Alex-EGF ligand in the microfluidic platform we have fabricated.

Within this microfluidic platform sequential ligand labeling, incubation, washing and fluorescent labeling are all carried out sequentially in a single nanoscale device. The volume of the reaction loop in this microfluidic platform is ca. 40 nL. Approximate 3.0 ng of EGF was consumed during the successful labeling and fluorescence imaging of cells in the four chambers. The successful use of these minute quantities of reagent demonstrates the practicability of using these types of microfluidic platforms to handle trace amounts of proteins in cellular research studies. Through the use of valves and pumps within our two-layer microfluidic system, different cell lines can be addressed into different chambers, individually immobilized, cultured, labeled, and imaged. The successful application of microfluidic chip design and utilization, described here, to fluorescent labeling identification of a growth factor receptor on target cells establishes a concept platform for performing cell sorting, cell incubation, and on-chip immunohistochemistry using extremely small amounts of cells or tissues. Moreover, these microfluidic chip operations are totally programmable; protein labeling, cell incubation with different media and reagents, and cell labeling can all be controlled using a computer. The entire process of ligand labeling, incubating probe with cells, washing and imaging is achievable within 30 min. When compared to studies with traditional Petri dish handling of cells and tissues, or even microwell analyses, experiments with the microfluidic platform described here are much less time consuming, conserve reagents, and are programmable, which makes these platforms a very promising new tool for biology studies.

Acknowledgments This research was supported by the UCLA In Vivo Cellular and Molecular Imaging Center (P50 CA086306:06), the UCLA Prostate SPORE (P50 CA092131:04) and institutional “start up” funds to HRT. GS acknowledges the support from UCLA-SOMI (Scholars

in Oncologic Molecular Imaging) program. The authors thank Prof. Stephen R. Quake from Stanford University for his kind help.

References

- V.C. Abraham, D.L. Taylor, and J.R. Haskins, *Trends Biotechnol.* **22**, 15–22 (2004).
- A. Aharonov, R. Pruss, and H. Herschman, *J. Cell. Biol.* **75**, A188 (1977).
- R.B. Bird, W.E. Stewart, and E.N. Lightfoot, *Transport Phenomena* (John Wiley & Sons, 2002).
- I. Braslavsky, B. Hebert, E. Kartalov, and S.R. Quake, *Proc. Nat. Acad. Sci. USA* **100**, 3960–3964 (2003).
- B.F. El-Rayes and P.M. LoRusso, *Brit. J. Cancer* **91**, 418–424 (2004).
- A. Groisman, M. Enzelberger, and S.R. Quake, *Science* **300**, 955–958 (2003).
- C.L. Hansen, M.O.A. Sommer, and S.R. Quake, *Proc. Nat. Acad. Sci. USA* **101**, 14431–14436 (2004).
- R.S. Herbst, *Int. J. Radiat. Oncol. Biol. Phys.* **59**, 21–26 (2004).
- P.J. Hung, P.J. Lee, P. Sabounchi, N. Aghdam, R. Lin, and L.P. Lee, *Biotechnol. Bioeng.* **89**, 1–8 (2005).
- J. Khandurina and A. Guttman, *Curr. Opin. Chem. Biol.* **6**, 359–366 (2002).
- C.C. Lee, G.D. Sui, A. Elizarov, C.Y.J. Shu, Y.S. Shin, A.N. Dooley, J. Huang, A. Daridon, P. Wyatt, D. Stout, H.C. Kolb, O.N. Witte, N. Satyamurthy, J.R. Heath, M.E. Phelps, S.R. Quake, and H.R. Tseng, *Science* **310**, 1793–1798 (2005).
- J. Liu, M. Enzelberger, and S. Quake, *Electrophoresis* **23**, 1531–1536 (2002).
- J. Liu, C. Hansen, and S.R. Quake, *Anal. Chem.* **75**, 4718–4723 (2003).
- J.C. McDonald and G.M. Whitesides, *Acc. Chem. Res.* **35**, 491–499 (2002).
- T.C. Merkel, V.I. Bondar, K. Nagai, B.D. Freeman, and I. Pinnau, *J. Polym. Sci. B-Polym. Phys.* **38**, 415–434 (2000).
- P. Nair, *Curr. Sci.* **88**, 890–898 (2005).
- R.M. Pruss and H.R. Herschman, *Proc. Nat. Acad. Sci. USA* **74**, 3918–3921 (1977).
- M.O. Reese, R.M. van Dam, A. Scherer, and S.R. Quake, *Genome Res.* **13**, 2348–2352 (2003).
- T. Thorsen, S.J. Maerkl, and S.R. Quake, *Science* **298**, 580–584 (2002).
- M.A. Unger, H.P. Chou, T. Thorsen, A. Scherer, and S.R. Quake, *Science* **288**, 113–116 (2000).
- P. Watts and S.J. Haswell, *Curr. Opin. Chem. Biol.* **7**, 380–387 (2003).
- O. Worz, K.P. Jackel, T. Richter, and A. Wolf, *Chem. Eng. Sci.* **56**, 1029–1033 (2001).